Computational and Structural Biotechnology Journal 20 (2022) 1366–1377

COMPUTATIONAL AND STRUCTURAL BIOTECHNOLOGY JOURNAL

journal homepage: www.elsevier.com/locate/csbj

Computer-aided engineering of staphylokinase toward enhanced affinity and selectivity for plasmin

Dmitri Nikitin [a,b,1], Jan Mican [a,b,e,1], Martin Toul [a,b,1], David Bednar [a,b], Michaela Peskova [c,g], Patricia Kittova [c,d], Sandra Thalerova [a,c,g], Jan Vitecek [a,c,e], Jiri Damborsky [a,b], Robert Mikulik [a,e], Sarel J. Fleishman [f], Zbynek Prokop [a,b,*], Martin Marek [a,b,*]

[a] International Clinical Research Center, St. Anne's University Hospital, Pekarska 53, 656 91 Brno, Czech Republic
[b] Loschmidt Laboratories, Department of Experimental Biology and RECETOX, Faculty of Science, Masaryk University, Kamenice 5, 625 00 Brno, Czech Republic
[c] Institute of Biophysics of the Czech Academy of Sciences, Kralovopolska 135, 612 65 Brno, Czech Republic
[d] Department of Biochemistry, Faculty of Medicine, Masaryk University, Kamenice 5, 625 00 Brno, Czech Republic
[e] Neurology Department, St. Anne's University Hospital and Faculty of Medicine, Masaryk University, Kamenice 5, 625 00 Brno, Czech Republic
[f] Weizmann Institute of Science, Rehovot 76100, Israel
[g] Department of Biochemistry, Faculty of Science, Masaryk University, Kamenice 5, 625 00 Brno, Czech Republic

ARTICLE INFO

Article history:
Received 15 December 2021
Received in revised form 2 March 2022
Accepted 5 March 2022
Available online 12 March 2022

Keywords:
Acute myocardial infarction
Stroke treatments
Thrombolytics
Plasminogen activators
Staphylokinase
Rational design
Affinity engineering
Enzyme kinetics
AffiLib

ABSTRACT

Cardio- and cerebrovascular diseases are leading causes of death and disability, resulting in one of the highest socio-economic burdens of any disease type. The discovery of bacterial and human plasminogen activators and their use as thrombolytic drugs have revolutionized treatment of these pathologies. Fibrin-specific agents have an advantage over non-specific factors because of lower rates of deleterious side effects. Specifically, staphylokinase (SAK) is a pharmacologically attractive indirect plasminogen activator protein of bacterial origin that forms stoichiometric noncovalent complexes with plasmin, promoting the conversion of plasminogen into plasmin. Here we report a computer-assisted re-design of the molecular surface of SAK to increase its affinity for plasmin. A set of computationally designed SAK mutants was produced recombinantly and biochemically characterized. Screening revealed a pharmacologically interesting SAK mutant with ~7-fold enhanced affinity toward plasmin, ~10-fold improved plasmin selectivity and moderately higher plasmin-generating efficiency *in vitro*. Collectively, the results obtained provide a framework for SAK engineering using computational affinity-design that could pave the way to next-generation of effective, highly selective, and less toxic thrombolytics.

1. Introduction

Acute myocardial infarction and ischemic stroke are lethal diseases that cause millions of deaths each year and leave many survivors disabled. In 2016, according to the World Health Organization, 17.9 million people died of cardiovascular diseases, with 85% of these deaths being caused by heart attacks and strokes. The occlusion of blood vessels by fibrin clots causes surrounding tissues to suffer from a lack of oxygen and nutrients, which can damage them irreversibly. Streptokinase, discovered in β-hemolytic streptococci in 1933, was the first thrombolytic factor capable of promoting enzymatic degradation of fibrin clots inside blood vessels [1]. This discovery was a huge advance because at that time acute myocardial infarctions could only be treated through complex surgery. When applied together with aspirin, the streptokinase infusions administered within a few hours of the onset of myocardial infarction halved mortality. Thrombolytics were introduced for stroke treatment in 1995 and have remained the first-line treatment ever since [2].

Two important plasminogen activators, urokinase and tissue plasminogen activator (tPA), were subsequently discovered in human urine and animal tissues, respectively [3,4]. Both are serine proteases that promote the conversion of plasminogen into active plasmin capable of degrading fibrin clots [5,6]. All three factors are

Abbreviations: SAK, Staphylokinase.

* Corresponding authors at: International Clinical Research Center, St. Anne's University Hospital, Pekarska 53, 656 91 Brno, Czech Republic.
E-mail addresses: zbynek@chemi.muni.cz (Z. Prokop), martin.marek@recetox.muni.cz (M. Marek).

[1] Shared first authors.

https://doi.org/10.1016/j.csbj.2022.03.004

still widely used to treat pathologies caused by blood vessel occlusions, generating annual revenues estimated to be in the billions of dollars.

The most widely used thrombolytic agent today is a recombinant tissue plasminogen activator (rtPA) known as alteplase, which has been approved by the Food and Drug Administration (FDA) for the treatment of ischemic stroke, acute myocardial infarction, and pulmonary embolism [2,7]. Due to its short plasma half-life and limited fibrin specificity, it does not provide reperfusion over 43% and causes bleeding complications in ~3–6% of stroke patients [8,9]. Moreover, its high cost restricts its use in low-income countries.

In contrast, staphylokinase (SAK) is an inexpensive indirect plasminogen activator first discovered in *Staphylococcus aureus* in 1948 [10]. It has a molecular weight of ~15.5 kDa and consists of only 136 amino acids [5,6]. It lacks enzymatic activity; instead, it changes the substrate specificity of plasmin, promoting the conversion of plasminogen into plasmin [11]. Its recombinant production is inexpensive, and it generates plasmin only on the fibrin surface [11]. The structure of its complex with partner and substrate microplasmin molecules has been determined by X-ray crystallography (PDB ID 1BUI) [12]. Because the activity of the SAK-plasmin complex is rapidly inhibited by α_2-antiplasmin, it can only convert plasminogen into plasmin in the vicinity of the fibrin clot surface, where it is protected from the inhibitory effect [11]. It also has a higher affinity for fibrin-bound plasminogen than for free plasminogen [13]. Consequently, SAK could be a safer thrombolytic agent than alteplase (rtPA).

SAK has been successfully tested in several clinical trials [14–16]. In the STAR trial, SAK and alteplase exhibited comparable efficacy with respect to early recanalization following acute myocardial infarction but SAK was significantly more fibrin-specific [14]. SAK42D (a natural isoform harboring four single-point mutations) and polyethylene glycol-modified (PEGylated) variants were successfully used in the Collaborative Angiographic Patency Trial of Recombinant Staphylokinase (CAPTORS) I and II in patients with acute myocardial infarction [15,16]. Both trials revealed clinically encouraging results of SAK application. There is also an ongoing phase 4 SAK clinical trial comparing ST-elevated acute myocardial infarction treatments to alteplase. To our knowledge, there are no published clinical trial results concerning the use of SAK for stroke treatment. One major drawback that limits the clinical usage of current SAK variants is their low affinity and selectivity for plasmin. Improving the affinity and selectivity of SAK should increase its residence time on plasmin, reducing the severity of side effects caused by unwanted *in vivo* interactions. Therefore, engineering the affinity and selectivity of SAK for plasmin could be a powerful way of improving its clinical usefulness.

Here, we report a structure-based mutagenesis study undertaken to increase the affinity of SAK for plasmin. We studied a number of previously reported SAK mutants including M26A, M26R, M26L, and Y44F [17] along with a number of newly-designed multiple-point mutants predicted by the recently developed AffiLib program [18]. Four of these designs, denoted SAK01, SAK02, SAK03, and SAK04, were selected for comprehensive biochemical and biological characterization. We performed a global kinetic analysis to identify the effects of each mutation on the individual steps of the SAK mechanism of action. The most promising SAK01 variant exhibited a ~7-fold increase in plasmin affinity, a ~10-fold increase in plasmin selectivity, and a slightly higher plasmin-generating efficiency *in vitro*. The SAK-wt and SAK01 variants were also compared to the clinically approved drug alteplase using *in vitro* clot models and showed superior or equivalent efficiencies.

2. Materials and methods

2.1. Structure preparation

The X-ray structure 1BUI [12] downloaded from RCSB PDB [19] contains the ternary complex between the "partner" microplasmin (chain A), the "substrate" microplasmin (chain B), and staphylokinase (chain C). Chains A and C were retained in all subsequent analyses. Residue numbering starts with Ser1, the first residue of staphylokinase excluding the signal peptide. Staphylokinase in the crystal structure differs from the wild-type sequence (UniProt [20] ID: P15240) by the following mutations: Gly34Ser, Arg36Gly, Arg43His. This three-point mutant structure was used as a starting point for the calculations.

2.2. Protein-protein interface optimization by AffiLib

The protein–protein interface was detected using the protein interface preset of PyMOL 2.1 [21] and optimized using the AffiLib web server [18]. The positions Tyr17, Tyr24, Met26, Asn28, Thr30, Thr71, Ala72, Thr90, Ile120, Asn126, and Ile128 were selected as positions to diversify. These positions represent the hydrophobic core of the interface (Fig. S1). The side chains of residues His43 and Tyr44 of staphylokinase were retained during the side chain optimization step of AffiLib because these residues are critical for binding plasminogen [22]. This resulted in a sequence space in which mutant structures were modeled. The sequence space was curated using a position-specific scoring matrix (PSSM) generated from a multiple sequence alignment of homologous sequences. The alignment was done by the web server using parameters of 30% minimal sequence identity, a maximum of 3000 sequences, minimal coverage of 60% length, and an E-value of 10^{-4}. Single point mutants having a PSSM score of −1.0 and lower were constructed in this sequence space. The energy of the single point mutants was evaluated, and less energetically favorable mutants, i.e. those with scores higher than the cutoff value of +2.0 Rosetta energy units (R.E.U.), were discarded. Finally, the mutations were combined into three- to five-point mutant structures, and the 50 highest scoring structures were made visible to the user.

2.3. Evaluation of thermostability

The thermostability of the top 50 structures from AffiLib was assessed with Rosetta 3.9 using protocol 16 as described by Kellogg and coworkers [23]. Structures were minimized with harmonic constraints placed on the Cα atoms in the crystal structure. The soft-repulsive design energy function was used for repacking side-chains. Optimization was performed on each whole protein without distance restriction. The previously created constraint files were then used for three rounds of backbone minimization with increasing weight on the repulsive term. The minimum energy from 50 iterations was used as the final parameter describing the thermodynamic stability (ΔΔG) of the multiple-point mutants. The stability was predicted as the difference in free energy of folding between the mutant protein and the wild-type (ΔΔG). A value of ΔΔG lower than 0 kcal.mol^{-1} indicates that the mutant protein is more thermodynamically stable then its corresponding wild type protein.

2.4. Construction of mutant proteins

A megaprimer protocol was used to construct staphylokinase single-point mutants. The mutagenic primers are listed in Table S1. The pET-for primer (5́-TAATACGACTCACTATAGGG-3́) and the N1-SAKxpET28b plasmid were used as a template to gen-

erate megaprimers that were subsequently purified on 0.8% agarose gels. Gel extraction was performed using a Nucleospin kit (Macherey-Nagel). The purified megaprimers were then used in mutagenic PCR with the N1-SAKxpET28b plasmid as a template. After transforming *Escherichia coli* DH5α cells with the PCR products and purifying candidate plasmids with a mini-scale plasmid purification kit (Macherey-Nagel, Germany), the N1-SAK M26A, M26R, M26L, and Y44F mutations were confirmed by sequencing. For the AffiLib-predicted SAK01, SAK02, SAK03, and SAK04 variants, genes bearing the multiple mutations described above were synthesized by GeneArt (ThermoFisher) and subcloned into the pET28b expression vector.

2.5. Protein expression and purification

Plasmids with genes coding for SAK variants M26A, M26R, M26L, Y44F, SAK01, SAK02, SAK03, and the SAK04 mutants were transferred into chemically competent *E. coli* BL21(DE3) cells. Grown colonies were inoculated into LB medium supplemented with kanamycin (50 μg mL^{-1}). The overnight cultures were diluted 100 times with fresh 2xLB medium containing kanamycin (50 μg mL^{-1}) and grown at 37 °C to OD_{600} ~0.6. Gene expression was then induced with 1 mM IPTG and cells were harvested after 3 h incubation at 37 °C by centrifugation. The cells were then resuspended in a buffer containing 20 mM Tris-HCl (pH 7.5) and 0.2 M NaCl, and stored at –20 °C.

The cells containing the M26A, M26R, M26L, Y44F, SAK01, SAK02, SAK03, and SAK04xpET28b proteins were disrupted by sonication with a Hielscher UP200S ultrasonic processor (Hielscher, Germany). Disrupted cells were centrifuged at 14,000 rpm for 1 h at 4 °C using a centrifuge (Laborzentriugen, Germany). The crude extracts were collected and applied on a Ni-NTA Superflow Cartridge column (Qiagen, Germany) in equilibration buffer (20 mM Tris-HCl, pH 7.5, 0.2 M NaCl, and 20 mM imidazole). The column was washed with 10 volumes of the equilibration buffer, and the target enzymes were eluted with a linear gradient of 20–250 mM imidazole. Protein peak fractions were then concentrated to 4–5 mL and loaded and purified on a Sephadex 16/60 S75 size-exclusion chromatography column. The purity of the proteins was evaluated by denaturing polyacrylamide gel electrophoresis (SDS-PAGE) and staining with Coomassie Brilliant Blue R-250 (Fluka, Switzerland). Protein concentrations were measured based on absorption at 280 nm using the following calculated extinction coefficients (M^{-1} cm^{-1}): wtSAK – 18910; M26A – 18910; M26R – 18910; M26L – 18910; Y44F – 17420; SAK01 – 18910; SAK02 – 18910; SAK03 – 20400; SAK04 – 18910. The pure protein fractions were pooled, flash-frozen in liquid nitrogen, and stored at −70 °C.

2.6. Fibrinolytic efficiency testing

SAK mutants' fibrinolytic properties were tested using fibrin plates. For this purpose, agar plates containing 1% agarose, 0.18% fibrin, 0.2 U mL^{-1} plasminogen, and 0.25 U mL^{-1} thrombin were prepared using PBS buffer, pH 7.4. Samples of interest (1–2 μL) were spotted in small holes on the surface of the agarized fibrin plates and incubated at 37 °C for several hours, making pictures on a dark background every 1 h. Buffers without proteins were used as negative controls. Diluted samples of the wild-type SAK were used as a positive control. For quantification, the diameter of the plate and the diameters of the clear fibrin-dissolved zones were determined using the ImageJ software (NIH and LOCI, USA) [24]. The diameters of the clear zones were squared and divided by the squared diameter of the whole plate to obtain the relative surface of the fibrin-dissolved zones at each time point (0% for no zone; 100% for the zone occupying the whole plate). For each SAK protein variant, the relative surface area was plotted against time, and the linear dependence of the zone growth was fit using a linear equation. The calculated slope provided information about the fibrinolytic activity in % of fibrin surface dissolved per hour. Finally, this value was normalized against the activity of SAK-wt, which was set to 1.0, to facilitate comparative analysis.

The plasminogen-activating efficiencies of the SAK variants were tested using a chromogenic substrate kit (AssayPro, USA) according to the manufacturer's instructions. Briefly, 60 μL of diluent, 10 μL of plasminogen, 10 μL of plasmin chromogenic substrate, and 20 μL of a sample of interest were mixed and the reaction was followed by an increase of absorbance at 405 nm while incubated at 37 °C. The buffer, containing 10 mM Tris-HCl (pH 7.5) and 50 mM NaCl, was used as a negative control.

2.7. Circular dichroism (CD) spectra and thermostability measurements

Samples of SAK mutants with final concentrations of 0.2 mg mL^{-1} were prepared in a buffer containing 10 mM Tris-HCl (pH 7.5) and 50 mM NaCl. CD spectra were obtained from 195 to 280 nm at 1 nm bandwidth with a 0.5 s integration time as an average of 5 readings using a Chirascan spectropolarimeter (Applied Photophysics, UK). Equilibrium denaturing curves were derived based on the ellipticity at 200, 210, and 220 nm, where the difference between the unfolded and native spectra was greatest. The temperature range was varied from 25 to 90 °C, with a temperature ramp of 1 °C min^{-1}. Melting curves were fitted using a sigmoid with slope model (Eq. (1)) where Θ_{MRE} corresponds to measured mean residue ellipticity at temperature T, Θ_{init} to initial mean residue ellipticity of a fully folded/native protein, Θ_{final} to final mean residue ellipticity of a fully unfolded protein, T_m to melting temperature of a protein, w to width of the sigmoid transition peak, and m to slope of the linear drift.

$$\Theta_{MRE} = \Theta_{init} + \frac{\Theta_{final} - \Theta_{init}}{1 + e^{\frac{T_m - T}{w}}} + m \cdot T \quad (1)$$

2.8. Surface plasmon resonance (SPR) affinity measurements

Biospecific interactions between the staphylokinase variants and plasmin were experimentally measured using a MP-SPR Navi 210A instrument (BioNavis, Finland). Plasmin was immobilized on the surface of an activated carboxymethyl dextran biosensor chip CMD200L via its amine groups using the EDC-NHS coupling method as recommended by the manufacturer. The coupling steps included (i) 7 min of surface cleaning using 2 M NaCl and 10 mM NaOH, (ii) 7 min of surface activation using a mixture of 50 mM N-hydroxysuccinimide (NHS) and 0.2 M N-(3-dimethylamino-propyl)-N-ethylcarbodiimide hydrochloride (EDC), (iii) 10 min of plasmin immobilization, and (iv) 5 min of surface deactivation using 1 M ethanolamine pH 8.0. A flow rate of 20 μL min^{-1} was used in all steps. Immobilization was performed in sodium acetate buffer (pH 4.5) using a final plasmin concentration of 20 μg mL^{-1}. The binding of each staphylokinase variant to the immobilized plasmin molecules was monitored at 25 °C in PBS pH 7.4 (10 mM Na_2HPO_4, 1.8 mM KH_2PO_4, 2.7 mM KCl, 137 mM NaCl). The association phase was initiated by injecting a staphylokinase variant for 5 min at a flow rate of 40 μL min^{-1}, then the dissociation phase was initiated by injecting pure buffer for 5 more minutes at the same flow rate. Regeneration of the chip and full release of the bound staphylokinase was accomplished by injecting 3 mM HCl for 2 min at a flow rate of 40 μL min^{-1}. The whole measurement cycle was repeated for each staphylokinase variant individually, applying several concentrations ranging from 0 to 50 μM to obtain the full concentration series. For plasminogen binding

measurements, the same protocol was followed with three minor adjustments: (i) a CMD50L biosensor chip was used to reduce the possibility of plasminogen cross-activation, (ii) the final plasminogen concentration during immobilization was 30 μg mL^{-1}, and (iii) staphylokinase variants' concentrations ranged from 0 to 65 μM.

2.9. Steady-state kinetics measurements

The kinetics of plasminogen activation were studied by recording changes in the fluorescence of the fluorogenic substrate D-VLK-AMC (AAT Bioquest, USA), which is processed by plasmin generated by plasminogen activators to form the fluorescent product 7-amino-4-methylcoumarin (AMC). The experiments were performed at 25 °C in phosphate-buffered saline PBS (pH 7.4) containing 1 mM $CaCl_2$. First, a staphylokinase variant was premixed with plasmin (Athens Research & Technology, USA) in a 1:1 ratio to preform the enzymatically active complex. After 30 min, 30 μL of D-VLK-AMC was mixed with 50 μL of various concentrations of plasminogen (Roche Diagnostics, Germany) inside a microplate well, followed by the addition of 20 μL of the premixed staphylokinase.-plasmin mixture to initiate the enzymatic reaction. The resulting concentrations in the reaction mixtures were 200 μM D-VLK-AMC, 6.2 nM staphylokinase variant, and 6.2 nM plasmin while the concentration of plasminogen ranged from 0 to 50 μM. Each measurement was performed in triplicate in three separated microplate wells of a black 96-well clear bottom microplate (PerkinElmer, USA). The plate was sealed with a transparent adhesive film to eliminate evaporation and the kinetics of plasminogen activation were monitored by recording the increase in fluorescence at 460 nm upon excitation at 360 nm using the microplate reader FLUOstar OPTIMA (BMG Labtech, Germany). For plasmin steady-state kinetics, the same protocol was applied but the reaction mixture consisted of 57 nM plasmin and D-VLK-AMC ranging from 0 to 600 μM.

2.10. Global numerical analysis of kinetic data

The analysis of kinetic data was performed by applying an updated protocol using global numeric fitting of raw kinetic data using KinTek Explorer 10 (KinTek Corporation, USA) [25–27]. This software allows for the input of a given kinetic model via a simple text description, and the program then derives the differential equations needed for numerical integration automatically. In the case of SPR affinity data, a previously proposed two-step induced-fit mechanism (Eq. (2)) was used as an input kinetic model. Eq. (3) was used to describe the results of the experiment involving an increasing SPR resonance signal (R) over time in response to the staphylokinase SAK variant binding to plasmin/ogen (Plm/Plg). For steady-state kinetics data, the measurements of the increasing fluorescence signal (F) over time upon enzymatic conversion were described using Eq. (4) based on the calibration curve of free fluorescent AMC. The steady-state model (Eqs. (5)–(7)) was used to obtain the values of the turnover number k_{cat}, and Michaelis constant K_m. A conservative estimate for diffusion-limited substrate binding (k_{+1} = 1000 $\mu M^{-1}.s^{-1}$) was used as a fixed value to mimic the rapid equilibrium assumption. Such arrangement makes the rate constant of product formation negligible compared to the rate constant of substrate release ($k_{-1} \gg k_{+2}$) and causes the Michaelis constant to be equal to the dissociation constant of the enzyme-substrate complex, as reflected in Eq. (7). All the kinetic data were fit globally and directly to the overall kinetic model depicted schematically in Fig. S3. Numerical integration of rate equations searching for a set of kinetic parameters that produce a minimum χ^2 value was performed using the Bulirsch–Stoer algorithm with adaptive step size, and nonlinear regression to fit the data was based on the Levenberg–Marquardt method. To account for fluctuations in the experimental data, plasminogen substrate concentrations were allowed to be slightly adjusted (±5%) to derive best fits. Residuals were normalized by sigma values for each data point. The standard error (S.E.) was calculated from the covariance matrix during nonlinear regression. A more rigorous analysis of the variation of the kinetic parameters was achieved by performing a confidence contour analysis using FitSpace Explorer (KinTek Corporation, USA). In these analyses, the lower and upper limits for each parameter were derived from the confidence contour by setting the χ^2 threshold at 0.95. The final fit provided a precise estimation of a total set of 10 kinetic constants for each staphylokinase variant.

$$\mathrm{Plm/Plg} + \mathrm{SAK} \underset{k_{-1}}{\overset{k_{+1}}{\rightleftarrows}} \mathrm{Plm/Plg.SAK} \underset{k_{-2}}{\overset{k_{+2}}{\rightleftarrows}} \mathrm{Plm/Plg^{*}.SAK} \tag{2}$$

$$\mathrm{R} = a \cdot \frac{\mathrm{Plm/Plg.SAK} + \mathrm{Plm/Plg^{*}.SAK}}{\mathrm{Plm/Plg} + \mathrm{Plm/Plg.SAK} + \mathrm{Plm/Plg^{*}.SAK}} \tag{3}$$

$$\mathrm{F} = A \cdot (1 - e^{-B \cdot [\mathrm{AMC}]}) + F_0 \tag{4}$$

$$\mathrm{SAK.Plm^{*}} + \mathrm{Plg} \underset{k_{-1}}{\overset{1000}{\rightleftarrows}} \mathrm{SAK.Plm^{*}.Plg} \overset{k_{+2}}{\rightarrow} \mathrm{SAK.Plm^{*}} + \mathrm{Plm} \tag{5}$$

$$k_{cat} = k_{+2} \tag{6}$$

$$K_m = \frac{k_{-1} + k_{+2}}{k_{+1}} \approx \frac{k_{-1}}{1000} \tag{7}$$

2.11. In vitro thrombolytic models

Thrombolytic experiments were performed using previously described static and flow *in vitro* models [28,29] that were optimized to determine the suitably measurable effect of alteplase in a highly repeatable manner as reported in previous publications [30,31]. Briefly, the static model consisted of 1.5 mL plastic tubes (Eppendorf, Germany) filled with medium to a total volume of 500 μL in which clots were individually incubated. Tubes were placed into a dry-block incubator at 37 °C and incubation lasted 60 min (the same amount of time indicated for alteplase treatment of stroke patients).

The flow model consisted of silicone chips (Sylgard 184 Silicone Elastomer, Dow Corning, USA) designed to mimic human middle cerebral artery anatomy, with narrowings based on dimensions seen in patient CT scans (n = 4). A bifurcation was included to enable permanent circulation in the system. Each silicone chip was connected by plastic pipes (internal diameter 3.1 mm) to an 8-channel pump head peristaltic pump (Gilson Minipuls 3, Gilson, Inc., USA) and the whole system was maintained at 37 °C for an incubation of 180 min. This arrangement maintained the hydrodynamic forces involved in clot removal [32], generating a pressure gradient of 10 mm Hg across the occlusion.

2.12. In vitro penetration microarray

Penetration experiments were performed in the microarray model outlined in recent publications [33–37] and optimized to determine the suitably measurable effect of alteplase in a highly repeatable manner. The microarray consisted of a micro-slide (μ-Slide VI 0.4, ibidi GmbH, Germany) into the channels of which a fibrin gel was prepared. Fluorescently labelled plasminogen activators or relevant fibrin non-interacting controls were applied to

individual micro-slide channels and the fluorescence intensity was continuously recorded at 5 min intervals for 180 min, at a distance of up to 1 mm from the application site (in 0.25 mm intervals), using a microscope (Nicon Eclipse TS 100, Zeiss AxioObserver Z1, Carl Zeiss AG, Germany) with fluorescent illumination from a metal halide fluorescence light source (HXP 120, Carl Zeiss AG, Germany) via a high efficiency filter set (Filter Set 43 HE (excitation BP 550/25; beam splitter FT 570; emission BP 605/70, Filter set 43 HE, Carl Zeiss AG, Germany).

2.13. Clots and fibrin gel preparation

Semi-synthetic clots were employed in both types of *in vitro* model. Clots were prepared from a mixture of human fibrinogen (Tisseel kit, Baxter, dissolved in water for injection to a concentration of 52 mg mL^{-1}), human thrombin (Tisseel kit, Baxter, dissolved in 40 μM $CaCl_2$ solution to a concentration of 3.3 IU mL^{-1} and red blood cells (RBCs) isolated from healthy donors' blood in a volumetric ratio of 1:1:1 by clotting in coated silicone chip fragments (for the flow model) or on parafilm (for the static model) for 30 min at 37 °C and >90% relative humidity under static conditions; prepared clots were immediately introduced into the model. The final concentration of components in prepared clots was 17.3 mg mL^{-1} fibrinogen, 1.1 IU mL^{-1} thrombin, and 4.17 × 10^9 RBCs mL^{-1}; the total clot volume was 90 μL for the static model and 60 μL for the flow model.

RBC dominant clots were prepared from 200 μL of healthy donors' whole blood without anticoagulant by clotting in borax glass tubes (inner diameter 8 mm) for 3.5 h at 37 °C and >90% relative humidity under static conditions; prepared clots were immediately introduced into the model.

Fibrin gel was prepared from the mixture of fibrinogen (Tisseel kit, Baxter, dissolved in water for injection to concentration 34.6 mg mL^{-1}) and thrombin (Tisseel kit, Baxter, dissolved in 40 μM $CaCl_2$ solution to concentration 2.2 IU mL^{-1}) in a volumetric ratio of 1:1 by clotting for 30 min in micro-slide channels at 37 °C and >90% relative humidity under static conditions. The final concentration of components in the prepared fibrin gel was 17.3 mg mL^{-1} fibrinogen and 1.1 IU mL^{-1} thrombin; the total volume per micro-slide channel was 30 μL.

All blood donors had agreed to donate blood samples, providing signed informed consent for the collection of blood. Individuals who had received acetylsalicylic acid, a non-steroidal anti-inflammatory, or antiplatelet drugs within 7 days before blood collection were excluded.

2.14. Plasminogen activators, fibrin non-interacting proteins and media preparation

Alteplase (Actilyse, Boehringer-Ingelheim International GmbH, Germany; Z. Nr. 1–24717) was dissolved in water for injection to a concentration of 1 mg mL^{-1} (for thrombolytic experiments) or 2 mg mL^{-1} (for penetration experiments) and was stored aliquoted at −20 °C (not re-frozen once thawed); it was then further diluted with PBS. The final concentration of alteplase was selected to be in line with clinically relevant dosing indicated for patients with ischemic stroke (1.3 μg mL^{-1}), according to the manufacturer's instructions and supporting pharmacokinetic data [38]. Wild type staphylokinase and the SAK01 mutant were dissolved in 10 mM Tris-HCl and 0.2 M NaCl buffer pH 7.5 to concentrations of 1.8 mg mL^{-1} and 1.1 mg mL^{-1}, respectively, and stored at 4 °C for up to 4 weeks. The final concentration of the staphylokinase variants was selected to be in line with the clinically relevant dosing of alteplase indicated for patients with ischemic stroke (1.3 μg mL^{-1}).

For penetration experiments, fibrin non-interacting proteins with similar molecular weights to the tested plasminogen activators were used as controls: bovine serum albumin (BSA, A9418, Sigma-Aldrich, USA) and α-lactalbumin from bovine milk (α-LA, L5385, Sigma-Aldrich, USA). BSA was dissolved in water for injection to a concentration of 2 mg mL^{-1} and stored at 4 °C for up to 4 weeks. α-LA was dissolved in 10 mM Tris-HCl and 0.2 M NaCl buffer pH 7.5 to a concentration of 2 mg mL^{-1} and stored at 4 °C for up to 4 weeks. Plasminogen activators and fibrin non-interacting proteins were fluorescently labelled prior to the penetration assay with rhodamine B isothiocyanate (283924, Sigma-Aldrich, USA), according to standard labeling protocol provided by the manufacturer. The final concentration of labelled plasminogen activators (and control proteins) was the same as for thrombolytic experiments, i.e. 1.3 μg mL^{-1}. The thrombolytic efficacy of the labelled plasminogen activators was verified in the static model (data not shown). All media were prepared using reagent grade chemicals. Plasma was used as the incubation environment in both models and was freshly prepared for each experiment from donors' citrated blood (in standard ratio of 3.8% sodium citrate: blood, 1:9) by centrifugation (500×g, 10 min, 4 °C) and kept at 4 °C prior to the experiment (up to 4 h).

2.15. Lytic efficacy testing

Clot lysis in the static model was determined by measuring clot mass loss [29–31,39] and by spectrophotometric determination of RBC release into the incubation media at 575 nm [30,31]. Clot lysis in the flow model was determined by measuring recanalization time, clot length, and spectrophotometric determination of RBC release [30]. Recanalization frequency was determined as a percentage ratio of complete recanalization to the total number of samples in the given treatment group. Relative clot reduction was determined as a percentage of clot area reduction before the release of the clot from the narrowed occlusion site. In addition, the thrombolysis rate was calculated using linear regression of relative clot reduction at 30 min intervals.

2.16. Penetration rate testing

Plasminogen activator penetration rate through fibrin was determined by continuous measurement of fluorescence intensities at a distance of up to 1 mm from the plasminogen activator application site front. The penetration rate was expressed as relative fluorescence intensity (RFI) at a given distance and time. RFI was determined using a custom image analysis script in the Python programming language. Penetration rate data were further standardized against the relevant control.

2.17. Data analysis and statistics

We expected relative clot mass loss in the static model to be 7 ± 6% for semi-synthetic clots and 24 ± 11% for RBC-dominant clots in the untreated group. Experiments were performed with 5 independent replicates for each clot type, giving us 80% statistical power to detect a relative clot mass loss of 18 ± 6% or more for semi-synthetic clots and 44 ± 11% or more for RBC-dominant clots in the treated group. All samples were processed in triplicate and in parallel. We expected the recanalization time in the flow model to be 180 ± 25 min in the untreated group. Five independent replicates were performed for each experiment, giving us 80% power to detect recanalization times of 132 ± 25 min or less in the treated group. All samples were processed in duplicate and in parallel. We expected the penetration rate to be 1.0 ± 0.2 in the control (BSA) group. Five independent replicates were conducted in each experiment, giving us 80% power to detect penetration rates of

0.6 ± 0.2 or less or 1.4 ± 0.2 or more in the treated group. All samples were processed in duplicate and in parallel. All analyses were performed with STATISTICA 12 (StatSoft) software. Data are expressed as means ± standard deviation if not otherwise indicated. The box plots show mean values (square), medians (lines), interquartile ranges (boxes), and minimum and maximum values (whiskers). Unpaired t-tests were used to compare data. P-values ≤ 0.05 were considered statistically significant.

3. Results and discussion

3.1. AffiLib prediction of improved SAK candidates

A set of 17,918 structures was generated with AffiLib using structural information on the SAK-microplasmin interface (Fig. S1) and the 50 best-scoring mutants were visually inspected for favorable interactions and evaluated for thermostability using Rosetta. Four mutants with favorable interactions were selected for further analysis (Table 1). Compared to the wild-type SAK-microplasmin complex, these structures all had: (i) longer side chains that were rich in hydrophobic amino acids, strengthening the desolvation effect of binding, (ii) more salt bridges and hydrogen bonds between the partner proteins, and (iii) more favorable AffiLib scores. Stability evaluations showed that some of the mutations in the chosen structures had destabilizing effects, so the corresponding designs would be expected to exhibit lower stability than the wild-type protein. The interfaces of the mutants selected for production are shown in Fig. 1.

3.2. Biochemical and functional characterization of SAK mutants

For our study, we selected the four best-scoring AffiLib designs (SAK01-04) SAK mutants and four previously studied mutants (SAK-M26A, SAK-M26R, SAK-M26L, and SAK-Y44F) carrying substitutions of key functional amino acids [40–42]. The proteins were purified from induced biomass using two-step affinity and size-exclusion chromatographies (see Materials and methods). As shown in Fig. S2, recombinantly produced SAK mutants were homogenously purified with yields of up to 40 mg per liter of bacterial culture. The yields of SAK03 and SAK04 were lower, up to 5 mg per 1 L of bacterial culture.

As shown in Fig. 2A and B, the circular dichroism (CD) spectra of the chosen SAK variants indicate that they generally folded correctly. The CD profiles of most of the SAK mutants resemble the wild-type SAK profile, although the profiles of SAK-M26L and SAK04 differed markedly from the native protein. It seems likely that the M26L substitution caused a serious CD shift (Fig. 2A, green line) and that these secondary structural changes were compensated by other amino acid substitutions in the SAK02, SAK03, and SAK04 variants (which also carry the M26L substitution). In the case of the SAK04 variant, the CD spectrum change appears to be related to partial unfolding.

Thermostability measurements (Fig. 2C, Fig. S3, Table S2) showed that the melting temperatures of the SAK-M26R and SAK-M26L variants were 2.75 °C higher and 2 °C lower than those of the wild-type SAK protein (60 °C), respectively. Even greater differences were observed among the AffiLib designs: the melting temperature of SAK02 was 2 °C higher than that of SAK-wt, whereas the melting temperatures of SAK01, SAK03, and SAK04 were reduced by 2.5 °C, 9.3 °C, and 13 °C, respectively. Chromogenic substrate and fibrin plate assays (Fig. S4A-C and Fig. 3) revealed that the SAK01, M26L, and Y44F variants had higher fibrinolytic efficiencies than SAK-wt but the other mutants were much less efficient.

3.3. Global kinetic analysis of the AffiLib designs of SAK

To determine the effects of the AffiLib-designed mutations on individual steps influencing the overall fibrinolytic activity and mechanism of action of SAK (Fig. S5), a global kinetic data analysis was performed (Fig. S6, Tables S3–5) as described previously [17]. This rigorous kinetic analysis allowed us to quantitatively characterize four key processes that determine the overall fibrinolytic effectivity of SAK variants (Fig. 3). A detailed description of the global data analysis, statistical details, and quantitative data on key processes is available in Supplementary Note 1. A detailed comparison of individual kinetic constants is provided in Supplementary Note 2.

The mutations of SAK02 and SAK03 exhibited no significant effects on plasmin and plasminogen binding, leading to only minor changes in plasmin selectivity when compared to SAK-wt. Furthermore, both SAK02 and SAK03 exhibited 3-fold reduced catalytic efficiencies, correlating well with their reduced overall fibrinolytic activities in the fibrin plate assay. The SAK04 mutations negatively affected binding to both plasmin and plasminogen but the effect on plasminogen was more pronounced, resulting in a slightly improved plasmin selectivity. However, the catalytic efficiency of SAK04 was 8% lower than that of SAK-wt, explaining its low overall fibrinolytic activity (Fig. 3).

Most significantly, the SAK01 variant exhibited a ~7-fold increase in affinity toward plasmin with a reduced affinity for plasminogen relative to the wild type. As a result, the selectivity for the formation of the active SAK01.plasmin complex was ~10-fold higher than for SAK-wt. The proposed mutations thus delivered the desired affinity increase but also reduced catalytic efficiency, leading to only a marginal improvement in overall fibrinolytic activity for SAK01.

3.4. Static model analysis of thrombolysis on in vitro clots

Treatment with all tested plasminogen activators provided greater clot mass loss ($p < 0.001$) and RBC release ($p < 0.001$) than in negative controls for both clot types (semi-synthetic and RBC-dominant). For semi-synthetic clots, alteplase showed lower clot mass loss ($p < 0.001$) and RBC release ($p < 0.001$) than SAK-wt, and similar clot mass loss ($p = 0.575$) and RBC release ($p = 0.233$) to SAK01. Additionally, SAK-wt induced greater thrombolysis than SAK01 (clot mass loss $p < 0.001$, RBC release $p = 0.006$). For RBC-dominant clots, alteplase caused lower clot mass loss ($p = 0.011$) but similar RBC release ($p = 0.157$) to SAK-wt, and similar clot mass loss ($p = 0.271$) and RBC release ($p = 0.588$) to SAK01. Both SAK proteins induced comparable levels of thrombolysis (clot mass loss $p = 0.163$, RBC release $p = 0.409$). These results are presented in more detail in Fig. 4, Fig. S7, and Table S6.

3.5. Flow model analysis of thrombolysis on in vitro clots

Treatment with all tested plasminogen activators reduced the recanalization time ($p < 0.001$), increased the recanalization frequency ($p < 0.001$) and RBC release ($p < 0.001$), reduced clot size ($p \leq 0.004$), and increased the thrombolysis rate ($p < 0.001$) when compared to the untreated group. Alteplase showed similar recanalization time ($p = 0.706$, $p = 0.049$), recanalization frequency ($p = 1.000$, $p = 1.000$), RBC release ($p = 0.996$, $p = 0.703$), relative clot reduction ($p = 0.362$, $p = 0.470$), and thrombolysis rate ($p = 0.918$, $p = 0.715$) as both SAK-wt and SAK01, respectively. Both SAK proteins had similar recanalization and thrombolysis parameters (recanalization time $p = 0.086$, recanalization frequency $p = 1.000$, RBC release $p = 0.692$, relative clot reduction $p = 0.914$, thrombolysis rate $p = 0.854$). The results obtained using the flow model are presented in more detail in Fig. 5, Fig. S8 and S9, and

Table 1
The SAK mutants chosen for further study, showing the amino acids at the diversified positions, the mutants' total scores according to AffiLib, and their predicted ΔΔG values obtained using protocol 16. The mutants are sorted according to their predicted score in Rosetta Energy Units (R.E.U). Mutated residues are shown in bold.

Name	Identity of diversified residues											Total Score [R. E. U.]	ΔΔG [kcal.mol-1]
	17	24	26	28	30	71	72	90	120	126	128		
SAK-wt	Y	Y	M	N	T	T	A	T	I	N	I	−974.3	0.0
SAK01	Y	Y	M	N	**I**	T	A	**Q**	**V**	**R**	I	−990.8	0.8
SAK02	Y	Y	**L**	N	T	**E**	A	T	**A**	**R**	**V**	−989.5	2.4
SAK03	Y	Y	**L**	N	**I**	**E**	A	**Y**	I	**V**	I	−989.5	−4.2
SAK04	Y	Y	**L**	**D**	T	**E**	A	**E**	**V**	N	I	−988.4	4.5

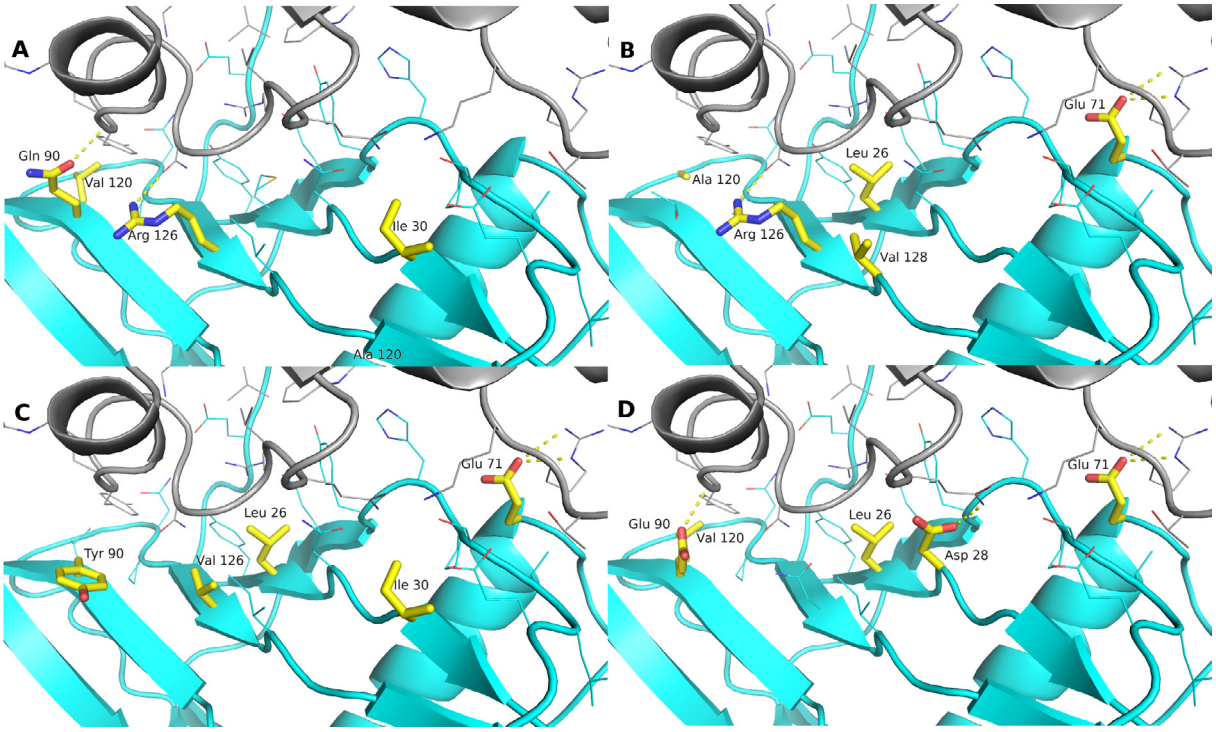

Fig. 1. Designed interfaces between the structures of staphylokinase (cyan) mutants SAK01–SAK04 (A–D, respectively) and partner microplasmin (grey) complexes. In the top-scoring structures, hydrophobic core residues and novel polar contacts are introduced. Mutated amino acids are shown as yellow sticks. Polar contacts between microplasmin and staphylokinase are shown as yellow dashed lines. Residues with new polar contacts between microplasmin and staphylokinase are shown as grey sticks, and the polar contacts as yellow dashed lines. (For interpretation of the references to colour in this figure legend, the reader is referred to the web version of this article.)

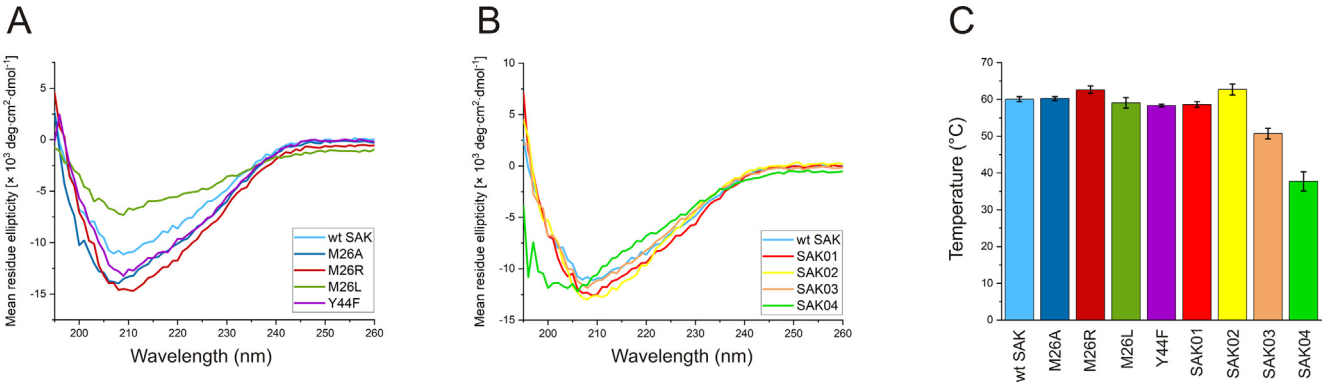

Fig. 2. Biophysical properties of SAK mutants. (A) CD spectra of the previously reported mutants M26A, M26R, M26L, and Y44F. (B) CD spectra of the AffiLib predicted designs SAK01–SAK04. (C) Melting temperatures of the previously reported mutants and AffiLib designs. The error bars represent a standard deviation from three replicates.

Table S7. In addition, clots treated with SAK-wt exhibited fragmentation: disintegration of clots into small pieces was observed in 67% of clots treated with SAK-wt but only in 10% of clots treated with SAK01, 0% of clots treated with alteplase and 0% in the untreated group.

3.6. Penetration microarray

All tested plasminogen activators caused detectable changes in the penetration rate when compared to a relevant fibrin non-interacting control. The initial normalized penetration rates (at a

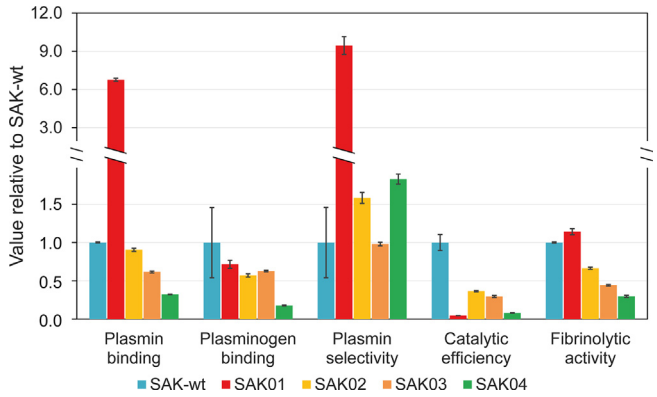

Fig. 3. Comparison of key parameters influencing the overall fibrinolytic effectivity of staphylokinase (SAK). The parameters include (i) formation of the active SAK.plasmin complex (plasmin binding), (ii) formation of the inactive SAK.plasminogen complex (plasminogen binding), (iii) selectivity for plasmin over plasminogen, and (iv) catalytic efficiency of the formed SAK.plasmin complex. The parameters were calculated as combinations of kinetic constants determined by global numerical analysis of kinetic data, as described in Supplementary Note 1. All kinetic experiments were performed in triplicate in phosphate-buffered saline PBS (pH 7.4) at 25 °C and the error bars represent standard deviations. For comparative purposes, the graph also includes the overall fibrinolytic activities for each variant determined by the fibrin plate assay.

distance of 0 mm) were as follows: bovine serum albumin (BSA) 1.0 ± 0.2, alteplase 0.6 ± 0.2 ($p = 0.001$), α-lactalbumin (α-LA) 1.0 ± 0.1, SAK-wt 1.9 ± 0.6 ($p < 0.001$), SAK01 1.7 ± 0.7 ($p = 0.003$). Alteplase had a significantly different penetration rate ($p < 0.050$) compared to the control (BSA) up to distances of 0.5 mm. Conversely, the penetration rates for SAK–wt and SAK01 only differed significantly from the control rate (α-LA) at the fibrin gel surface (0 mm), ($p \leq 0.003$); at distances further from the surface, their rates were similar to the control ($p \geq 0.050$). These results are presented in more detail in Fig. 6.

3.7. Comparison of previously reported data with our results

We selected a number of previously reported single point mutants and subjected them to deep structural and functional testing. Residue methionine 26 (M26) was previously established to be responsible for high-affinity binding to plasminogen [40]. Specifically, it was shown that the inactive M26A and M26R SAK mutants exhibited 10–20-fold lower association affinity constants for plasminogen binding than SAK-wt. Our results indicated that M26R retains some weak plasmin-generating activity, but M26A completely lacks such activity (Fig. S4A and C). The M26V substitution caused almost complete inactivation of the protein [41]. Interestingly, introducing a leucine residue with a non-polar sidechain bulkier than those of alanine and valine markedly changed the protein's functional and structural properties: the M26L mutant was not only functional but had a higher plasmin-generating efficiency than the wild-type SAK in both the chromogenic substrate and the fibrin plate assays (Fig. S4A-C). This mutant was previously reported to be as active as the wild type [41]. The presence of the bulky hydrophobic amino acid at position 26 affected the protein's secondary structure, as indicated by a comparison of its CD spectrum to that of the wild type, but did not reduce its stability (Fig. 2A and C).

Tyrosine 44 (Y44) and histidine 43 (H43) were proposed to contribute to cation-π and π-π interactions with the tryptophan 215 (W215) residue of plasmin [43]. According to the Dahiya and coworkers, the Y44F mutant was almost as efficient as the wild type SAK protein (k_{cat} = 0.40 and 0.43 s^{-1}, respectively). In our chromogenic substrate assay, this mutant was much less productive in plasmin generation than wild type SAK (Fig. S4A), but slightly outperformed it in the fibrin plate assay (Fig. S4C). This single amino acid mutation had neutral effects on the protein's secondary structure and stability.

The results of our melting temperature estimation experiments were somewhat inconsistent with previous reports [42]. In particular, an earlier publication claimed melting temperatures of 43.7 and 43.5 °C for wild-type SAK and the M26L variant, respectively. In contrast, we estimated them to be 60 and 58 °C. These differences could be explained by differences in buffer composition, sample preparation, and instrument choice.

3.8. The AffiLib-designed staphylokinase variant SAK01 outperforms wild-type SAK in plasmin affinity and selectivity

Despite intensive efforts in SAK engineering, to our knowledge the single and multiple amino acid mutations studied so far have all reduced or completely eliminated the protein's capacity to generate plasmin. To avoid such problems, we used a recently devel-

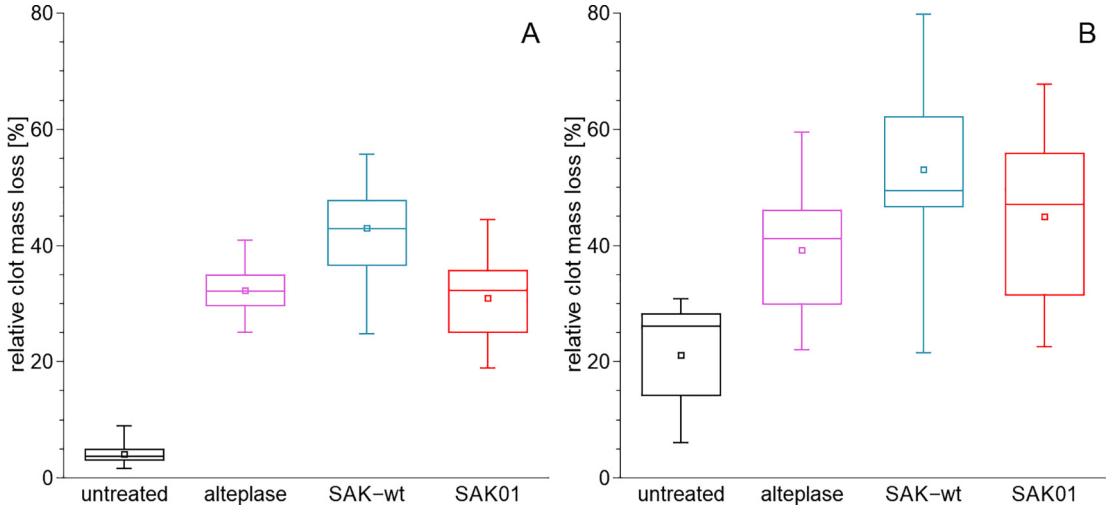

Fig. 4. Clot lysis in a static model expressed as relative clot mass loss. (A) semi-synthetic clots, N = 15. (B) RBC dominant clots, N = 15. The box plots show mean values (squares), medians (lines), interquartile ranges (boxes), and minimum and maximum values (whiskers). The plotted results show that treatment with the tested plasminogen activators (alteplase, SAK-wt, SAK01) induced efficient thrombolysis. Alteplase induced a lower level of thrombolysis than SAK-wt and a similar level to SAK01.

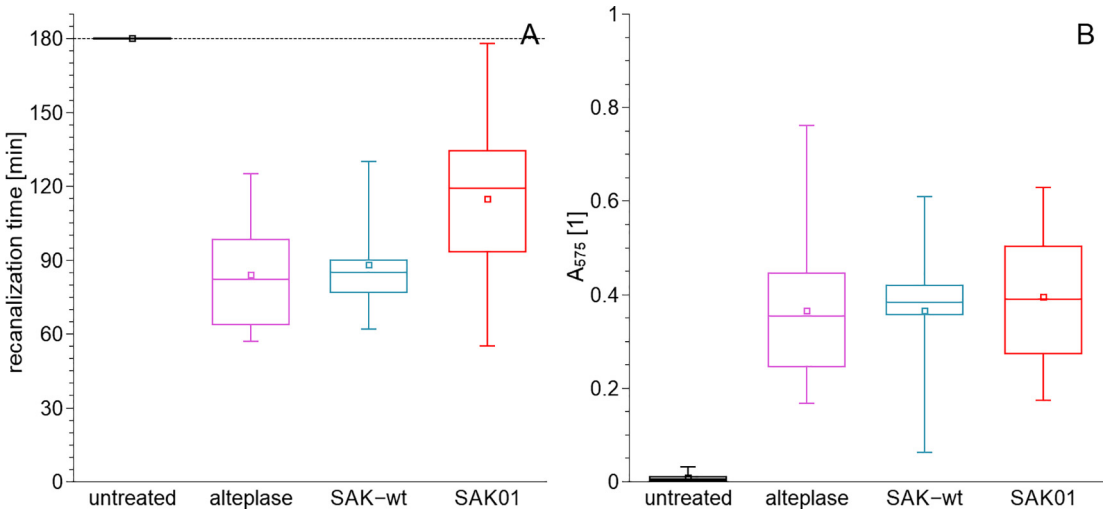

Fig. 5. Clot lysis in a flow model. (A) recanalization time. (B) RBC release, N = 10. The box plots show mean values (square), medians (lines), interquartile ranges (boxes), and minimum and maximum values (whiskers). The dashed line shows the experimental time window (180 min). The plotted results show that treatment with the tested plasminogen activators (alteplase, SAK-wt, SAK01) led to efficient recanalization and increased the thrombolysis rate. Alteplase had similar effects on recanalization and thrombolysis to SAK-wt and SAK01.

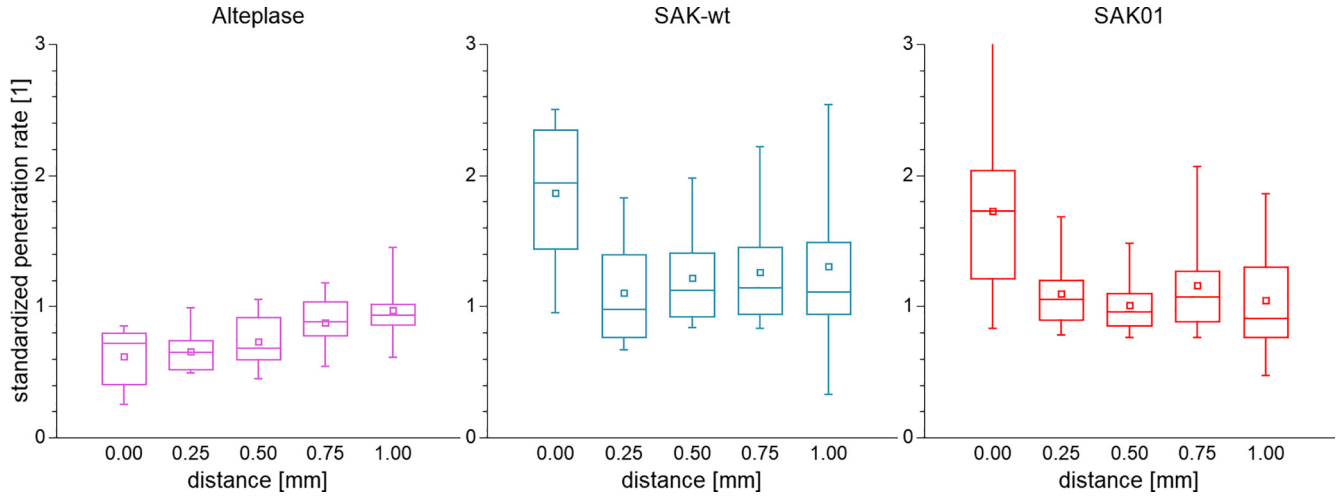

Fig. 6. Penetration rates for alteplase, SAK-wt, and SAK01, determined using a penetration microarray, N = 10–12. The box plots show mean values (squares), medians (lines), interquartile ranges (boxes), and minimum and maximum values (whiskers). The rates are standardized against the rates for relevant fibrin non-interacting controls, namely bovine serum albumin for alteplase and α-lactalbumin for SAKs. The tested plasminogen activators exhibited clearly and measurably different penetration rates compared to relevant controls, at least close to the surface (at a distance of 0 mm). Alteplase was significantly hindered in the gel relative to the control at distances of up to 0.5 mm, whereas the SAKs penetrated without being hindered.

oped algorithm implemented in AffiLib [18] to predict multiple-mutation SAK variants with increased plasmin affinity based on the previously reported crystal structure of SAK in complex with two microplasmin molecules [12]. This algorithm takes into account pre-organized polar interaction networks responsible for high specificity to create synthetic interaction networks. Using this rational design approach, we predicted and selected four SAK multiple amino acid mutants that were predicted to have superior plasmin-binding properties (Fig. 1). We hypothesized that these variants might outperform the wild-type protein by promoting thrombolysis at lower concentrations with shorter reperfusion times.

Recent publications have highlighted the value of drug-target residence time as a predictor of future *in vivo* efficacy [44,45]. The clinical profile of SAK could thus be improved by increasing its drug-target residence time. In particular, such an increase could reduce side-effects arising from binding to other receptors, including immunogenic responses induced by binding to immune cells or dissolving physiological hemostatic clots. Increasing the resistance of SAK to being washed out of the clot could also enhance the effectivity of thrombolysis. Finally, SAK mutants with improved affinity could be retained in clot fragments for a longer time after clot fragmentation, which could prevent re-occlusions, a major complication of thrombolysis in the clinic [46,47]. All these processes could lead to a more effective and safer thrombolytic treatment. Furthermore, it was previously shown that inefficient binding to plasmin is the main factor limiting overall staphylokinase effectivity, making the rational improvement of SAK's affinity for plasmin a highly desirable goal [17].

SAK is a small protein of 136 amino acids. As a result, it is difficult to use mutagenesis to improve one of its properties without detrimental effects on others. In our case, multiple amino acid substitutions reduced the protein's stability (Fig. 2). Particularly severe losses of stability were observed for the SAK03 and SAK04 variants.

In biological assays, only SAK01 slightly outperformed the native protein in both the chromogenic substrate and the fibrin plate assays (Fig. 3, Fig. S4B and C).

An advanced global kinetic data analysis protocol was applied to the constructed mutants SAK01–SAK04, allowing analysis of the effects of mutations on individual steps of SAK's mechanism of action. SAK02 and SAK03 exhibited no significant change in plasmin and plasminogen affinity but their catalytic efficiency was reduced 3-fold compared to the wild-type (Fig. 3, Fig. S5, Tables S3–S5). SAK04 yielded reduced affinity to both plasmin and plasminogen, leading to slightly improved plasmin selectivity. However, the catalytic efficiency dropped more than 10-fold, in keeping with this variant's low overall fibrinolytic activity. SAK01 exhibited ∼7-fold improved plasmin affinity and ∼10-fold increased plasmin selectivity. However, its catalytic efficiency was 5% of that for SAK-wt, resulting in comparable overall fibrinolytic activity. Computational design using AffiLib thus successfully improved selectivity for plasmin binding and yielded an interesting variant, SAK01. An improved plasmin affinity would be expected to increase the drug-target residence time, potentially improving the overall clinical profile of SAK even though the variant's fibrinolytic activity is comparable to that of the wild type protein.

3.9. In vitro clot assay comparison of alteplase, SAK-wt, and SAK01

In vitro thrombolysis assays were conducted to compare the efficacy of SAK-wt and SAK01 to that of alteplase (the current standard for stroke treatment) when applied to *in vitro* clots prepared from human blood or its components. Static and flow *in vitro* models were developed and used for functional characterization of SAK-wt and SAK01. Clots were incubated in human plasma, mimicking the native environment of thrombolysis, in particular the high abundance of plasminogen and other fibrinolytic activators and inhibitors. The limitations of these models, including the absence of an excretory system, paradoxically ensured a sufficient supply of fibrinolytic factors without the need for continual supplementation of fresh plasma. The concentrations of alteplase and SAKs were set to levels reflecting the therapeutic doses of alteplase used in stroke patients [38]. Additionally, a penetration microarray was conducted to study the penetration rate of the chosen plasminogen activators through a fibrin network mimicking a blood clot.

In the static model (high plasminogen concentration) with semi-synthetic clots, SAK-wt induced a higher degree of thrombolysis than alteplase and SAK01, as indicated by rates of both clot mass loss and RBC release. On the other hand, with RBC-dominated clots, increased thrombolysis was apparent only in measurements of clot mass loss. All of the tested plasminogen activators yielded similar results with regards to RBC release. The fact that clot mass loss mediated by SAKs did not correlate with RBC release suggests that the mechanism of action of SAK and its variants differs from that of alteplase, for which the amount of released RBCs correlates closely with the relative clot mass loss in the long term [30,31]. The greater loss of clot mass following treatment with SAK-wt suggests that clot lysis proceeded mainly in the fibrin component, while RBCs remained densely packed in the remaining clot. The high penetration capability and relatively low plasmin affinity of SAK-wt could lead to rapid clot penetration followed by fibrin degradation inside the clot [5,6]. However, SAK01 has a ∼7-fold higher affinity for plasmin than SAK-wt; this might be expected to limit its penetration into clots, explaining its lower thrombolytic efficacy in the static model. In the flow model (with high plasminogen levels), there were no statistically significant differences between the studied thrombolytic enzymes with respect to recanalization and thrombolysis. This suggests that hydromechanical forces may cause unbound SAK-wt to penetrate through the clot too rapidly. The increased plasmin affinity of SAK01 could prevent its leaching from the clot. In accordance with the higher thrombolytic efficacy of SAK-wt observed in the static model, this protein induced clot fragmentation in 67% of cases in the flow model. Conversely, fragmentation was never seen with alteplase (0% of cases) and rarely with SAK01 (10% of cases). These results again suggest that the mechanism of action of alteplase in the presence of high plasminogen concentrations differs from that of SAK-wt and its variants because alteplase has limited ability to penetrate into clots. The higher clot fragmentation rates observed with the two SAK variants could potentially be helpful for preventing reocclusion in clinical applications.

Penetration capability through the fibrin network was evaluated using a penetration microarray in the presence of low plasminogen concentrations. Under such conditions, the formation of complexes between SAKs and plasmin is apparently limited. Therefore, the assay monitors mainly the fibrin-SAK interaction. Alteplase showed a significantly lower penetration rate than the control protein BSA, indicating a substantial level of binding within the fibrin network [5,6,48]. Conversely, the penetration rates of SAK-wt and SAK01 did not differ from the control. We speculate that this could be due to the limited supply of plasminogen in the microarray, suggesting a plasmin and/or plasminogen dependency of SAKs [5,6,49,50]. Both SAKs accumulated in the surface layer of the fibrin network and then penetrated at the same rate as the non-interacting control protein α-LA, suggesting a weak interaction with fibrin.

4. Conclusion

We performed a detailed characterization of the biophysical and functional properties of the previously reported SAK variants M26A, M26R, M26L, and Y44F along with four new AffiLib-predicted mutants. Global kinetic analysis and an analysis of *in vitro* clot thrombolytic efficiency revealed that the variant SAK01 exhibited 7-fold increased plasmin binding affinity and 10-fold increased plasmin selectivity compared to wild-type SAK. This improvement confirmed the success of the computational design strategy, which aimed to improve protein–protein interactions between SAK and plasmin. SAK01 was shown to retain the overall fibrinolytic activity of SAK-wt and its thrombolytic efficiency towards *in vitro* clots while greatly reducing its main clinical limitation of inefficient plasmin binding. A protein with a potentially superior clinical profile has thus been identified and could serve as a valuable starting point for further computational design efforts or directed evolution studies seeking to improve its catalytic efficiency. These results also constitute a proof-of-concept of a strategy for designing thrombolytic drugs that can be used at lower dosages while having longer half-lives, shorter reperfusion times, and negligible side effects when compared to currently used treatments.

CRediT authorship contribution statement

Dmitri Nikitin: Investigation, Formal analysis, Visualization, Writing – original draft. **Jan Mican:** Investigation, Formal analysis, Visualization, Writing – original draft. **Martin Toul:** Investigation, Formal analysis, Visualization, Writing – original draft. **David Bednar:** Conceptualization, Supervision, Methodology, Writing – review & editing. **Michaela Peskova:** Investigation, Formal analysis, Visualization, Writing – original draft. **Patricia Kittova:** Investigation, Formal analysis, Visualization, Writing – original draft. **Sandra Thalerova:** Investigation, Formal analysis, Visualization, Writing – original draft. **Jan Vitecek:** Conceptualization, Supervi-

sion, Methodology, Writing – review & editing. **Jiri Damborsky:** Conceptualization, Supervision, Funding acquisition, Writing – review & editing. **Robert Mikulik:** Conceptualization, Methodology. **Sarel J. Fleishman:** Conceptualization, Supervision, Methodology. **Zbynek Prokop:** Conceptualization, Supervision, Methodology. **Martin Marek:** Conceptualization, Supervision, Methodology, Writing – review & editing.

Declaration of Competing Interest

The authors declare that they have no known competing financial interests or personal relationships that could have appeared to influence the work reported in this paper.

Acknowledgements

The authors would like to express their thanks for financial support to the European Regional Development Fund – Project INBIO (CZ. 02.1.01/0.0/0.0/16_026/0008451). Martin Toul and Sandra Thalerova are supported by the scholarship Brno Ph.D. Talent. CIISB research infrastructure project LM2018127 funded by MEYS CR is gratefully acknowledged for the financial support of the measurements at the CF Nanobio and CF BIC. Computational resources were supplied by the project "e-Infrastruktura CZ" (e-INFRA CZ LM2018140) supported by the Ministry of Education, Youth and Sports of the Czech Republic, and by the ELIXIR-CZ project (LM2018131), part of the international ELIXIR infrastructure.

Ethical approval

This article does not contain any studies with human participants or animals performed by any of the authors.

Appendix A. Supplementary data

Supplementary data to this article can be found online at https://doi.org/10.1016/j.csbj.2022.03.004.

References

[1] Tillett WS, Garner RL. The fibrinolytic activity of hemolytic streptococci. J Exp Med 1933;58:485–502.
[2] Sila CA, Furlan AJ. Therapy for acute ischemic stroke: the door opens. Interpreting the NINDS rt-PA stroke study. Cleve Clin J Med 1996;63:77–9.
[3] Macfarlane RG, Pilling J. Fibrinolytic activity of normal urine. Nature 1947;159:779.
[4] Rijken DC, Wijngaards G, Zaal-de Jong M, Welbergen J. Purification and partial characterization of plasminogen activator from human uterine tissue. Biochim Biophys Acta 1979;580:140–53.
[5] Mican J, Toul M, Bednar D, Damborsky J. Structural biology and protein engineering of thrombolytics. Comput Struct Biotechnol J 2019;17:917–38.
[6] Nikitin D, Choi S, Mican J, Toul M, Ryu W-S, Damborsky J, et al. Development and testing of thrombolytics in stroke. J Stroke 2021;23(1):12–36.
[7] Collen D, Lijnen HR. The tissue-type plasminogen activator story. Arterioscler Thromb Vasc Biol 2009;29:1151–5.
[8] Bivard A, Huang X, Levi CR, Spratt N, Campbell BC, et al. Tenecteplase in ischemic stroke offers improved recanalization: analysis of 2 trials. Neurology 2017;89:62–7.
[9] Yaghi S, Willey JZ, Cucchiara B, Goldstein JN, Gonzales NR, Khatri P, et al. Treatment and outcome of hemorrhagic transformation after intravenous alteplase in acute ischemic stroke: A scientific statement for healthcare professionals from the American Heart Association/American Stroke Association. Stroke 2017;48:e343–61.
[10] Lack CH. Staphylokinase; an activator of plasma protease. Nature 1948;161:559.
[11] Collen D. Staphylokinase: a potent, uniquely fibrin-selective thrombolytic agent. Nat Med 1998;4:279–84.
[12] Parry MA, Fernandez-Catalan C, Bergner A, Huber R, Hopfner KP, et al. The ternary microplasmin-staphylokinase-microplasmin complex is a proteinase-cofactor-substrate complex in action. Nat Struct Biol 1998;5:917–23.
[13] Sakharov DV, Lijnen HR, Rijken DC. Interactions between staphylokinase, plasmin(ogen), and fibrin. Staphylokinase discriminates between free plasminogen and plasminogen bound to partially degraded fibrin. J Biol Chem 1996;271:27912–8.
[14] Vanderschueren S, Barrios L, Kerdsinchai P, Van den Heuvel P, Hermans L, et al. A randomized trial of recombinant staphylokinase versus alteplase for coronary artery patency in acute myocardial infarction. The STAR Trial Group. Circulation 1995 15;;92(8):2044–9.
[15] Armstrong PW, Burton J, Pakola S, Molhoek PG, Betriu A, et al. Collaborative angiographic patency trial of recombinant staphylokinase (CAPTORS II). Am Heart J 2003;146:484–8.
[16] Armstrong PW, Burton JR, Palisaitis D, Thompson CR, Van de Werf F, et al. Collaborative angiographic patency trial of recombinant staphylokinase (CAPTORS). Am Heart J 2000;139:820–3.
[17] Toul M, Nikitin D, Marek M, Damborsky J, Prokop Z. Extended mechanism of the plasminogen activator staphylokinase revealed by global kinetic analysis: 1000-fold higher catalytic activity than That of clinically used alteplase. ACS Catal 2022;12:3807–14.
[18] Netzer R, Listov D, Lipsh R, Dym O, Albeck S, et al. Ultrahigh specificity in a network of computationally designed protein-interaction pairs. Nat Commun 2018;9:5286.
[19] Berman HM, Westbrook J, Feng Z, Gilliland G, Bhat TN, et al. The protein data bank. Nucleic Acids Res 2000;28:235–42.
[20] The UniProt Consortium. UniProt: the universal protein knowledgebase in 2021. Nucleic Acids Res 2021;49:D480–9.
[21] Schrödinger, LLC. The PyMOL Molecular Graphics System, Version 2.1 2015.
[22] Singh S, Ashish DKL. Pro(42) and Val(45) of staphylokinase modulate intermolecular interactions of His(43)-Tyr(44) pair and specificity of staphylokinase-plasmin activator complex. Febs Lett 2012;586:653–8.
[23] Kellogg EH, Leaver-Fay A, Baker D. Role of conformational sampling in computing mutation-induced changes in protein structure and stability. Proteins Struct Funct Bioinform 2011;79:830–8.
[24] Schneider CA, Rasband WS, Eliceiri KW. NIH image to ImageJ: 25 years of image analysis. Nat Methods 2012;9(7):671–5.
[25] Johnson KA, Simpson ZB, Blom T. Global Kinetic Explorer: a new computer program for dynamic simulation and fitting of kinetic data. Anal Biochem 2009;387:20–9.
[26] Johnson KA, Simpson ZB, Blom T. FitSpace Explorer: an algorithm to evaluate multi-dimensional parameter space in fitting kinetic data. Anal Biochem 2009;387:30–41.
[27] Johnson KA. Fitting enzyme kinetic data with KinTek global kinetic explorer. Comp Methods Enzymol 2009;467:601–26.
[28] Harpaz D, Chen X, Francis CW, Marder VJ, Meltzer RS. Ultrasound enhancement of thrombolysis and reperfusion in vitro. J Am Coll Cardiol 1993;6:1507–11.
[29] Prasad S, Kashyap RS, Deopujari JY, Purohit HJ, Taori GM, Daginawala HF. Development of an in vitro model to study clot lysis activity of thrombolytic drugs. Thromb J 2006;4:14.
[30] Thalerová S, Pešková M, Kittová P, Gulati S, Víteček J, Kubala L, et al. Effect of apixaban pretreatment on alteplase-induced thrombolysis: an in vitro study. Front Pharmacol 2021;12:740930.
[31] Víteček J, Vítečková Wünschová A, Thalerová S, Gulati S, Kubala L, et al. Factors influencing recombinant tissue plasminogen activator efficacy: an in vitro study. Life Sci 2021. in submission.
[32] Diamond SL. Engineering design of optimal strategies for blood clot dissolution. Annu Rev Biomed Eng 1999;1:427–62.
[33] Rottenberger Z, Komorowicz E, Szabó L, Bóta A, Varga Z, et al. Lytic and mechanical stability of clots composed of fibrin and blood vessel wall components. J Thromb Haemost 2013;11:529–38.
[34] Marcos-Contreras OA, Ganguly K, Yamamoto A, Shlansky-Goldberg R, Cines DB, Muzykantov VR, et al. Clot penetration and retention by plasminogen activators promote fibrinolysis. Biochem Pharmacol 2013;85:216–22.
[35] Longstaff C. Measuring fibrinolysis: from research to routine diagnostic assays. J Thromb Haemost 2018;16:652–62.
[36] Longstaff C, Varjú I, Sótonyi P, Szabó L, Krumrey M, et al. Mechanical stability and fibrinolytic resistance of clots containing fibrin, DNA, and histones. J Biol Chem 2013;288:6946–56.
[37] Morrow GB, Whyte CS, Mutch NJ. Functional plasminogen activator inhibitor 1 is retained on the activated platelet membrane following platelet activation. Haematologica 2020;105:2824–33.
[38] Acheampong P, Ford GA. Pharmacokinetics of alteplase in the treatment of ischaemic stroke. Expert Opin Drug Metab Toxicol 2012;8:271–81.
[39] Elnager A, Abdullah WZ, Hassan R, Idris Z, Arfah NW, Sulaiman SA, et al. In vitro whole blood clot lysis for fibrinolytic activity study using D-dimer and confocal microscopy. Adv Hematol 2014;2014:814684.
[40] Lijnen HR, De Cock F, Van Hoef B, Schlott B, Collen D. Characterization of the interaction between plasminogen and staphylokinase. Eur J Biochem 1994;224(1):143–9.
[41] Schlott B, Hartmann M, Gührs KH, Birch-Hirschfeld E, Gase A, Vettermann S, et al. Functional properties of recombinant staphylokinase variants obtained by site-specific mutagenesis of methionine-26. Biochim Biophys Acta 1994;1204(2):235–42.
[42] Dornberger U, Fandrei D, Backmann J, Hübner W, Rahmelow K, Gührs KH, et al. A correlation between thermal stability and structural features of staphylokinase and selected mutants: a Fourier-transform infrared study. Biochim Biophys Acta 1996;1294(2):168–76.

[43] Dahiya M, Singh S, Rajamohan G, Sethi D, Dikshit A. Intermolecular interactions in staphylokinase-plasmin(ogen) bimolecular complex: function of His43 and Tyr44 FEBS Lett 2011; 585:1814.
[44] Lee KS, Yang J, Niu J, Ng CJ, Wagner KM, et al. Drug-target residence time affects in vivo target occupancy through multiple pathways. ACS Cent Sci 2019;5:1614–24.
[45] Copeland RA. The drug–target residence time model: a 10-year retrospective. Nat Rev Drug Discov 2016;15:87–95.
[46] Leach JK, Patterson E, O'Rear EA. Distributed intraclot thrombolysis: mechanism of accelerated thrombolysis with encapsulated plasminogen activators. J Thromb Haemost 2004;2:1548–55.
[47] Alexandrov A, Grotta J. Arterial reocclusion in stroke patients treated with intravenous tissue plasminogen activator. Neurology 2002;59(6):862–7.
[48] Knuttinen MG, Emmanuel N, Isa F, Rogers AW, Gaba RC, Bui JT, et al. Review of pharmacology and physiology in thrombolysis interventions. Semin Intervent Radiol 2010;27:374–83.
[49] Baruah DB, Dash RN, Chaudhari MR, Kadam SS. Plasminogen activators: a comparison. Vascul Pharmacol 2006;44:1–9.
[50] Nedaeinia R, Faraji H, Javanmard SH, Ferns GS, Ghayour-Mobarhan M, et al. Bacterial staphylokinase as a promising third-generation drug in the treatment for vascular occlusion. Mol Biol Rep 2020;47:819–41.